Chemistry–A European Journal
Research Article
doi.org/10.1002/chem.202402244
Chemistry Europe
European Chemical Societies Publishing
www.chemeurj.org

Hot Paper

Superior Tumor Cell Uptake by Mono- and Tri-Nuclear Rhodamine-Gadolinium(III) Agents

Amy G. Robertson,[a] Andrew J. Hall,[a] Anita Marfavi,[a, b] and Louis M. Rendina*[a, b]

The synthesis and characterization of a novel trinuclear rhodamine-Gd(III) complex, along with two analogous mononuclear rhodamine-Gd(III) complexes, are reported. All complexes displayed good selectivity in a human glioma cell line (T98G) when compared to a glial cell line (SVG p12), with low cytotoxicities. Superior tumor cell uptake for these Gd(III) complexes was observed at lower incubation concentrations compared to previously-reported delocalized lipophilic cations such as a rhodamine-lanthanoid(III) probe and Gd(III)-arylphosphonium complexes, with *ca.* 150% and 250% increases in Gd uptake, respectively.

Introduction

With the prevalence of cancer expected to rise world-wide, there is an increased demand in developing novel cancer therapeutics and diagnostic tools. In particular, new strategies are necessary to combat highly aggressive and malignant cancers of the brain, such as glioblastoma (GBM), where patient prognosis and median survival time (<2 years) are especially poor.[1]

The mitochondria play a critical role in normal cellular metabolic processes, as well as in necrotic and apoptotic cell death pathways.[2,3] An important distinction between normal cell and cancer cell mitochondria is the significantly elevated mitochondrial trans-membrane potential ($\Delta\Psi_m$) in the latter. This difference in membrane potential provides a suitable avenue for developing specific mitochondrial-targeting therapeutics and molecular imaging probes.

Delocalised lipophilic cations (DLC) are useful mitochondrial-targeting agents, with >100-fold selectivity towards cancer cell mitochondria.[4] Many DLCs may also exhibit fluorescent properties due to their rigid, conjugated aromatic ring system. Hence, there exists a plethora of applications for DLCs including fluorescence imaging,[5,6] and targeted drug delivery.[7,8]

Commonly investigated DLCs include arylphosphonium salts, F16 and Rhodamine 123 (Figure 1).[9,10] Current DLC-based agents, namely the arylphosphonium salts, including tetraphenylphosphonium (TPP) and triphenylmethylphosphonium (TPMP), have drawn significant interest and attention due to their inherently lower toxicity compared to other DLCs.[11,12] Furthermore, rhodamine dyes are known to display high mitochondrial uptake, and hence provide a unique avenue to be investigated as DLCs to enhance tumor cell uptake and selectivity. Notably, rhodamine compounds are typically reliant on a delocalised positive charge for uptake by tumor cell mitochondria, which is influenced by the position of equilibrium in lactone formation, resulting in greater mitochondrial uptake in the cationic form.[13,14]

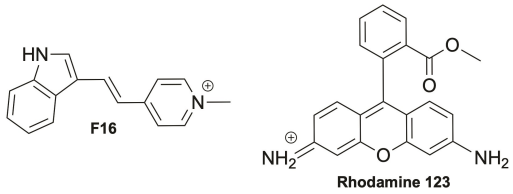

Figure 1. Common delocalised lipophilic cations (DLC).

Due to its highly paramagnetic nature, Gd(III) plays a prominent role in medicine as a key component in magnetic resonance imaging (MRI) contrast agents. Approximately 40% of all MRI scans utilize these agents,[15] with those Gd contrast agents currently approved for clinical use possess one of two general ligand structures; (a) linear, for example Gd-DPTA (Magnevist®) or (b) macrocyclic, such as Dotarem®. Theranostic effects have focused on macrocyclic ligands due to their greater thermodynamic stability with lanthanoid metal ions and, thus, result in a reduced loss of non-toxic Gd^{3+} ions.[16] Notably, there is an increasing surge in interest in the use of Gd agents in gadolinium neutron capture therapy (GdNCT) as ^{157}Gd (natural abundance = 15.7%) contains the highest thermal capture cross section (254,000 barns) for all naturally-occurring elements, and is *ca.* 66-fold greater than ^{10}B (3800 barns), the dominant NCT isotope.[17] Furthermore, due to its large *K*-edge (50.2 keV),[18] Gd is also an excellent candidate for photon activation therapy (PAT), whereby irradiation utilizes a synchrotron X-ray beam, rather than the (epi)thermal neutrons used in NCT, which can radiosensitize the Gd aggregated within tumor cells to

[a] *A. G. Robertson, A. J. Hall, A. Marfavi, L. M. Rendina*
School of Chemistry, The University of Sydney, Sydney, NSW 2006, Australia
E-mail: louis.rendina@sydney.edu.au
[b] *A. Marfavi, L. M. Rendina*
Nano Institute, Sydney, NSW 2006, Australia

Supporting information for this article is available on the WWW under https://doi.org/10.1002/chem.202402244

ultimately achieve a therapeutic effect with the release of high-energy Auger and Coster-Kronig (ACK) electrons.[19,20]

Previously-reported Gd(III)-DLCs have focussed primarily on the arylphosphonium series due to their selective accumulation within mitochondria and high tumor cell uptake.[12,21–23] Rivas and co-workers have previously reported multimodal MRI/fluorescent probes containing a Rhodamine B group and a lanthanoid (Gd and/or Tb)-complexed DOTA macrocycle. The Gd(III) agent was the first example of a small-molecule MRI/fluorescent probe displaying an 'off-on' pH switching response with preferential uptake in tumor cells, although intracellular Gd levels were not determined in this study.[24] Herein we report the synthesis and characterisation of three new rhodamine-based Gd(III) complexes, and report key parameters including lipophilicity, cellular uptake in foetal glial (SVG p12) and human glioblastoma (T98G) cells, in addition to the fluorescence properties of selected compounds. One key consideration in the design of new rhodamine-based probes was the nature of the linker between the rhodamine core and the DO3A macrocycle, as this factor would likely impact both the fluorescence properties as well as their cellular uptake and tumor cell selectivity.

Results and Discussion

In this work, three new rhodamine-Gd(III) agents (**RG-A1**, **RG-A2**, **RG-A3**, Scheme 1) were synthesised using a multi-step synthetic procedure. Modifications to the nature of the linker were implemented whereby the inclusion of linear amine-based linkers (hydrazine or alkyl amine) or a cyclic linker (piperazine) were assessed. The initial synthesis of the linear-based complexes utilised Rhodamine B (**1**) and Rhodamine 6G (**3**), bridged using a hydrazine or ethylenediamine, respectively, promoting lactone formation in compounds **4** and **5**.[25] The subsequent synthetic step involved synthesis of the acetyl chloride derivatives (**6** and **7**) using chloroacetyl chloride and K_2CO_3. Coupling of the rhodamine fragments to the DO3A macrocycle was then performed using DO3A-^{t}Bu$_3$·HBr in the presence of K_2CO_3 in MeCN, to afford compounds **8** and **9**. Removal of the *tert*-butyl protecting groups from the DO3A macrocycle was successfully achieved by using a 1:1 mixture of TFA and DCM (**10** and **11**). The macrocyclic ligands were then purified by means of reverse-phase HPLC which were isolated in >95% purity. Characterisation of the deprotected ligands (**10** and **11**) was primarily achieved by means of MALDI-TOF mass spectrometry. Finally, Gd(III) complexation reactions were performed using a suspension of Gd_2O_3 in H_2O, removal by filtration of excess Gd_2O_3, and subsequent lyophilisation of compounds **RG-A1** and the trinuclear complex **RG-A2**. Compound **RG-A3** was synthesized in a similar manner to that described for **RG-A1** and **RG-A2** in Scheme 1, with two key differences: (a) the initial step involved piperazine ring incorporation with Rhodamine B base **2**, $AlMe_3$ and piperazine in DCM;[26] and (b) DO3A complexation was performed in DCM instead of MeCN which was found to improve the rate of reaction and yield. The identities of the three complexes were confirmed by means of MALDI-TOF MS, with loss of the single coordinated H_2O molecule observed due to ionization.[27]

Cell viabilities of healthy glial SVG p12 and the human glioblastoma T98G cell lines were determined by means of a 3-[4,5-dimethylthiazol-2-yl]-2,5-diphenyltetrazolium bromide (MTT) assay,[28] assessing the half-maximal inhibitory concentration (IC_{50}) of the Gd(III) complexes (**RG-A1**, **RG-A2**, and **RG-A3**) over the concentration range of 1 mM–31.25 μM (**Table S1**). The complexes were assessed against the related rhodamine-Gd(III) derivative (**Gd·L2**, **Figure S7**) reported by Rivas and coworkers,[24] as well as previously-reported phosphonium derivatives.[21,23] All compounds displayed low cytotoxicities ($IC_{50} > 0.5$ mM) when compared to known theranostic agents (e.g. Motexafin-Gd) and free rhodamine dyes.[23] The IC_{50} value of compound **RG-A3** displayed the lowest cytotoxicity (1.0 mM). It is worth noting that these IC_{50} values are *ca.* 1.0 mM higher than previously reported Gd(III)-phosphonium-based compounds.[21,23] The nature of the rhodamine counter-ion has also been shown to increase cytotoxicity.[29]

Due to the lipophilic nature of cell and mitochondrial membranes, it is crucial to determine the lipophilicity of Gd(III) complexes as a key parameter in explaining cell uptake trends. As such, the lipophilicity ($\log D_{7.4}$) of compounds **RG-A1**, **RG-A2**, and **RG-A3** were determined at pH 7.4 (Table 1). The lipophilicity data shows noteworthy trends to those of previously reported Gd(III)-arylphosphonium derivatives, whereby **RG-A1** and **RG-A2** were found to more hydrophilic, but **RG-A3** was more lipophilic, that many of these agents.[21,23] All complexes displayed excellent lipophilicities for future *in vivo* studies with $\log D_{7.4}$ values lying between *ca.* 1–3.

In vitro cell uptake studies of rhodamine-Gd(III) complexes **RG-A1**, **RG-A2**, and **RG-A3** in SVG p12 and T98G cell lines were assessed at four different concentrations (31.25 μM–250 μM) by means of ICP-MS which measured the total Gd content of cells. Cell uptake selectivities expressed as tumor to normal (T/N)

Table 1. Lipophilicity and cellular uptake in SVG p12 and T98G cells of compounds **RG-A1**, **RG-A2**, and **RG-A3**.

Complex	Log$D_{7.4}$	Conc. (μM)	SVG p12 (ng Gd/mg protein)	T98G (ng Gd/mg protein)	T/N[a]
RG–A1	0.94 ± 0.14	31.25	243 ± 47	1710 ± 212	7.0
		62.5	2048 ± 538	4432 ± 957	2.2
		125	1983 ± 73	2806 ± 522	1.4
		250	1756 ± 160	1705 ± 191	1.0
RG–A2	1.04 ± 0.15	31.25	230 ± 62	1568 ± 196	6.8
		62.5	3862 ± 533	5116 ± 209	1.3
		125	1905 ± 356	2101 ± 211	1.1
		250	1401 ± 172	1459 ± 161	1.0
RG–A3	2.53 ± 0.15	31.25	91 ± 4	533 ± 94	5.8
		62.5	345 ± 18	1317 ± 195	3.8
		125	1224 ± 222	1642 ± 102	1.3
		250	5047 ± 534	6531 ± 750	1.3

[a] T/N = tumor/normal cell ratio.

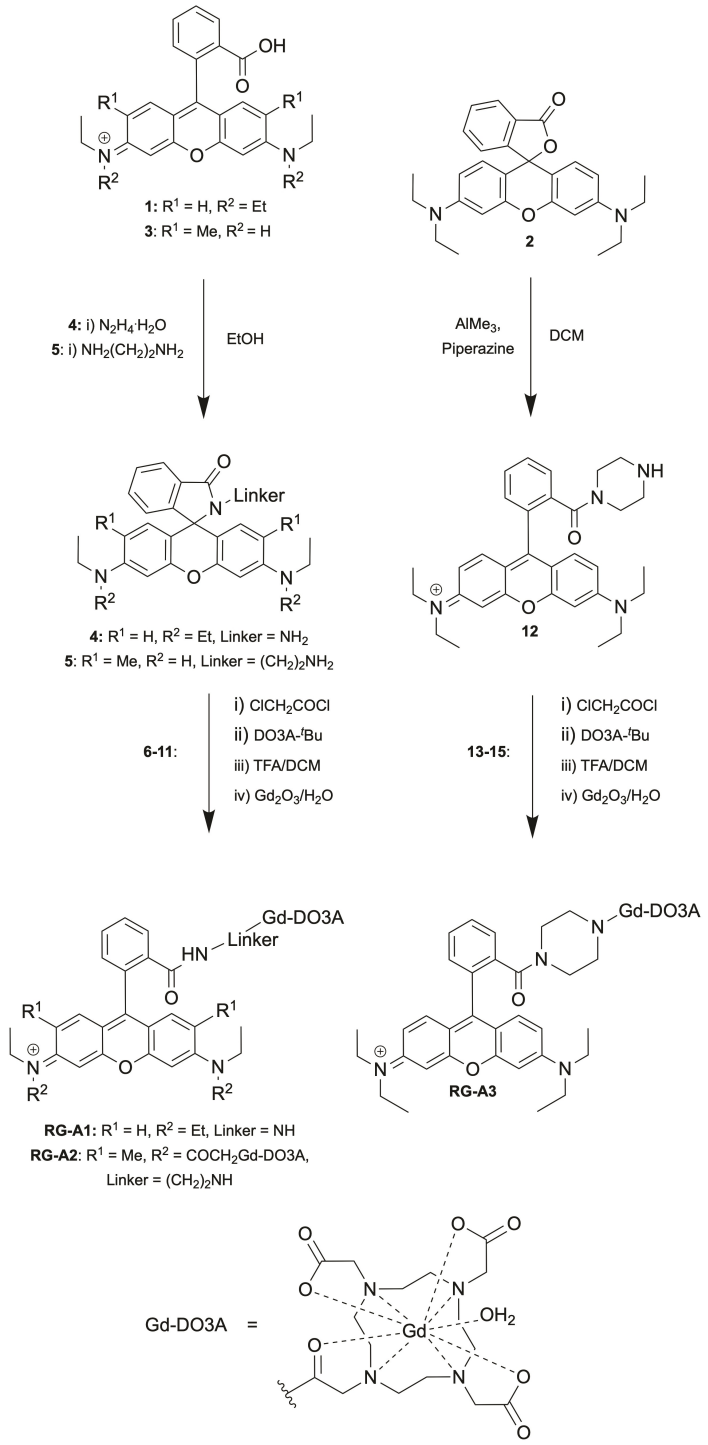

Scheme 1. Synthesis of rhodamine-Gd(III) complexes **RG-A1**, **RG-A2**, and **RG-A3** (for clarity, the acetate counter-ions are not shown).

ratios are presented in Table 1. These results demonstrate a significantly greater uptake of rhodamine-Gd(III) complexes at low incubation doses (i.e. <62.5 μM). Notably, at 31.25 μM, all complexes displayed statistically-significant selectivity for glioma over glial cells, with superior selectivity (T/N ~1.5 fold greater) compared to a previously-reported dual-imaging Gd(III) probe.[24] Remarkably, the tumor cell uptake of the trinuclear Gd(III) complex **RG-A2** was found to be *ca.* 250% greater than that of previously reported arylphosphonium-Gd(III) salts at 62.5 μM,[21] with an cell uptake of 5116 ng Gd/mg protein. Between the two linear-linked amine complexes (**RG-A1** and **RG-A2**), the carbohydrazide linked derivative **RG-A1** displayed the highest uptake in the T98G cell line at most of the assessed Gd incubation concentrations (except at 62.5 μM). Complex **RG-A1** also showed superior selectivity at 31.25 μM, with a T/N of 7.0, likely due to the favoured equilibrium position of the

Table 2. Spectroscopic properties of the parent Rhodamine B (**1**) and rhodamine-Gd(III) complexes **RG-A1** and **RG-A3** in 0.1 M HCl (pH 1).

Compound	λ_{ex} (nm)	λ_{em} (nm)	Stokes Shift (nm)	τ_f (ns)	Φ_f
1	558	577	19	1.58	0.24
RG-A1	561	582	21	1.57	0.09
RG-A3	560	596	36	2.82	0.15

lactone form. Notably, in the case of complex **RG-A2**, there was no major advantage observed in tumor cell delivery of Gd despite it being a trinuclear complex. Whereas the Gd levels at all concentrations were found to be high for this particular complex, such levels were found to be similar to those determined for the mononuclear complexes **RG-A1** and **RG-A3**, and certainly was found to be lower than the anticipated 3-fold higher levels expected as a consequence of the 3:1 ratio of Gd atoms/molecule in **RG-A2**. It is most likely that the large molecular dimensions of **RG-A2** limit its cell and mitochondrial membrane permeability, leading to a decreased Gd uptake.

To assess the photophysical properties of the Gd(III) complexes, including absorption, emission, fluorescence lifetime (τ_f), and quantum yield (Φ_f) were examined (Table 2). The probes were dissolved in 0.1 M HCl to ensure the fluorescence properties of the cationic dyes were measured rather than the uncharged lactone form. Notably, the trinuclear Gd(III) complex **RG-A2** did not exhibit any detectable fluorescence, most likely due to extensive quenching of the chromophores due to the heavy atom effect and paramagnetism of the three Gd(III) centres which promotes singlet-triplet intersystem crossing and, therefore, reduces fluorescence intensity.[30] In contrast, complexes **RG-A1** and **RG-A3** displayed red-shifts in both the excitation and emission profiles compared to the parent Rhodamine B (**1**, $\lambda_{ex} = 558$ nm and $\lambda_{em} = 577$ nm).[31] The inclusion of a piperazine linker in complex **RG-A3** generated the largest bathochromic shift (λ_{em} increase by 20 nm, as compared to Rhodamine B). The piperazine-based complex also displayed a *ca.* 2-fold increase in fluorescence lifetime compared to the carbohydrazide-linked complex **RG-A1**. The quantum yield of complex **RG-A3** was also higher than that of **RG-A1** ($\Phi_f = 0.15$ and 0.09, respectively). The differences in photophysical properties for both compounds suggests that the nature of the linker is an important determinant in these cases. It is well-documented that azacyclic linkers such as piperazine in complex **RG-A3** impart greater chain stability than linear linkers due to the enhanced rigidity of the ring due to the presence of the nitrogen atom.[32,33] This reduced flexibility prevents the rhodamine scaffold entering into a twisted intramolecular charge transfer (TICT) state, hence enhancing the fluorescence lifetime and quantum yield.

Conclusions

In conclusion, three new rhodamine-based Gd(III) agents **RG-A1**, **RG-A2**, and **RG-A3** were synthesised and characterised, two mononuclear and one trinuclear complex, with the fluorescent properties of the mononuclear compounds assessed. All complexes displayed low *in vitro* cytotoxicity in healthy (SVG p12) and tumor (T98G) cell lines. Furthermore, the determined lipophilicities of the three complexes were found to be suitable for applications in biological systems ($\log D_{7.4}$ = *ca.* 1.0–3.0). Superior tumor cell uptake was observed at lower concentrations compared to previously a reported mononuclear rhodamine-Gd(III) probe[24] and other DLCs such as Gd(III)-phosphonium complexes,[21] with *ca.* 150% and 250% increases in Gd uptake, respectively, found for complex **RG-A2** at 62.5 μM. Moreover, the greatest uptake T/N selectivity was determined to be 7:1 at a concentration of 31.25 μM in the case of complex **RG-A1**. Reasonable quantum yields and fluorescence lifetimes were also observed for compounds **RG-A1** and **RG-A3**, but the trinuclear complex **RG-A2** did not exhibit any detectable fluorescence. Both complexes **RG-A1** and **RG-A3** displayed bathochromic shifts in the excitation and emission profiles as compared to the parent Rhodamine B dye. The rhodamine-Gd(III) complexes prepared in this work are promising agents to guide the future design of new tumor theranostics. Future studies including *in vivo* animal studies to determine toxicity, tumor uptake, and pharmacokinetics will be reported in due course.

Experimental Section

General experimental details and instrumentation are provided in the Supporting Information. Compounds **5** and **12** were prepared according to the literature procedures.[25,26] The general stepwise procedures for the synthesis of the rhodamine-Gd(III) complexes prepared in this work are presented below.

Rhodamine B hydrazide (**4**): A solution of amine (1.0 eq) in ethanol (30 mL) was prepared. Hydrazine hydrate (14 eq) was then added dropwise with vigorous stirring at room temperature. The solution was heated to reflux for 4–5 h or until the solution changed from dark pink to light orange. The mixture was cooled and the solvent was removed under reduced pressure. 1 M HCl (50 mL) was added to the solid, generating a clear red solution. 1.0 M NaOH (70 mL) was added dropwise until the pH reached 9–10. The resulting precipitate was filtered to afford the desired hydrazide intermediate. Compound **4**: Isolated yield: 1.16 g (94%). ^{1}H NMR (300 MHz, CD_3CN): δ 1.1 (t, 12H, $J = 7.4$), 3.30–3.37 (q, 8H, $J = 6.94$), 6.35–6.41 (m, 6H), 6.94–7 (m, 1H), 7.45–7.5 (m, 2H), 7.78–7.85 (m, 1H). MALDI-TOF MS for $[M]^+$: calculated *m/z* 457.260, observed *m/z* 457.237.

Acetyl chloride synthesis (**6**, **7**, and **13**): The amine (1.0 eq, **4**, **5**, or **12**) was dissolved in dry DCM (50 mL) with K_2CO_3 (9.0 eq) and the solution was cooled to 0 °C on ice. Chloroacetyl chloride (9.0 eq) was then added dropwise, and the solution was stirred for a further 30 mins at 0 °C, warmed to room temperature, and then stirred for 4 h. The solution was then filtered and removed under reduced pressure. The crude solid was dissolved in DCM (50 mL), washed with H_2O (3×50 mL) and then brine (3×50 mL). The solution was dried with sodium sulfate, filtered, and solvent removed to yield the corresponding acid chloride intermediates. Compound **6**: Isolated yield: 0.9 g (82%). MALDI-TOF MS for $[M]^+$: calculated *m/z* 533.230, observed *m/z* 533.229. Compound **7**: Isolated yield: 0.632 g (54%); MALDI-TOF MS for $[M]^+$: calculated *m/z* 685.180, observed *m/z* 685.129. Compound **13**: Isolated yield: 0.722 g (81%); MALDI-TOF MS for $[M]^+$: calculated *m/z* 587.280, observed *m/z* 587.299.

DO3A coupling (**10**, **11**, **15**): The acid chloride derivative (1.0 eq, **6**, **7**, or **13**) was stirred in MeCN (50 mL) with DO3A-(^{t}Bu$_3$)·HBr (1.1 eq; 3.5 eq for **11**) and K_2CO_3 (19 eq) for 48 h or until reaction completion (as determined my MALDI-TOF MS). The solution was then filtered and the solvent was removed. DCM (3 mL) and TFA (3 mL) were subsequently added and the mixture was left to stir for 18 h before removing the solvent under nitrogen. The resulting solid was dissolved in Milli-Q H_2O before purification by HPLC. Compound **10**: Yield: 15 mg (12%); MALDI-TOF MS for $[M]^+$: calculated *m/z* 843.440, observed *m/z* 843.496. Compound **11**: Yield: 38 mg (5%); MALDI-TOF MS for $[M]^+$: calculated *m/z* 1559.740, observed *m/z* 1559.738. Compound **15**: Yield: 15 mg (18%); MALDI-TOF MS for $[M]^+$: calculated *m/z* 989.550, observed *m/z* 989.549.

Gd(III) complexation (**RG-A1**, **RG-A2**, **RG-A3**): Excess Gd_2O_3 (2.3 eq; 5.2 eq for **RG-A2**) was added to a solution of the deprotected ligand (1.0 eq) dissolved in DMF (3 mL, **10**) or H_2O (3 mL, **11** or **14**). The mixture was stirred at room temperature for 72 h before the removal of residual Gd_2O_3 by centrifugation and subsequent filtration through a 0.2 μM PTFE syringe filter. The solution was then lyophilized to afford the pure Gd(III) complex. Compound **RG-A1**: Yield: 11 mg (93%); >95% purity by HPLC. MALDI-TOF MS for $[M–H_2O]^+$: calculated *m/z* 998.342, observed *m/z* 998.342. Compound **RG-A2**: Yield: 60 mg (93%); >95% purity by HPLC. MALDI-TOF MS for $[M–3H_2O]^+$: calculated *m/z* 2079.505, observed *m/z* 2079.320. Compound **RG-A3**: Yield: 45 mg (96%); >95% purity by HPLC. MALDI-TOF MS for $[M–H_2O]^+$: calculated *m/z* 1052.389, observed *m/z* 1052.407.

Supporting Information Summary

General experimental details and instrumentation, MALDI-TOF mass spectra, HPLC traces, and *in vitro* cytotoxicity data of Gd(III) complexes.

Acknowledgements

We acknowledge the Australian Government for a Research Training Program Scholarship awarded to AGR. LMR is grateful for funding from the Australian Research Council (DP190103461). This research was facilitated by access to Sydney Analytical, a core research facility at The University of Sydney. Open Access publishing facilitated by The University of Sydney, as part of the Wiley - The University of Sydney agreement via the Council of Australian University Librarians.

Conflict of Interests

There are no conflicts of interest to declare.

Data Availability Statement

The data that support the findings of this study are available in the Supporting Information of this article.

Keywords: Gadolinium · Imaging agents · Rhodamine dyes · Mitochondrial-targeting · Tumor uptake

[1] A. C. Tan, D. M. Ashley, G. Y. López, M. Malinzak, H. S. Friedman, M. Khasraw, *CA: A Cancer J. Clin.* **2020**, *70*, 299–312.
[2] E. Vringer, S. W. G. Tait, *Cell Death Differentiation* **2023**, *30*, 304–312.
[3] W. Chen, H. Zhao, Y. Li, *Signal. Transduct. Target Ther.* **2023**, *8*, 333.
[4] H. Chen, J. Wang, X. Feng, M. Zhu, S. Hoffmann, A. Hsu, K. Qian, D. Huang, F. Zhao, W. Liu, H. Zhang, Z. Cheng, *Chem. Sci.* **2019**, *10*, 7946–7951.
[5] K. Qian, H. Chen, C. Qu, J. Qi, B. Du, T. Ko, Z. Xiang, M. Kandawa-Schulz, Y. Wang, Z. Cheng, *Nanomed. Nanotechnol. Biol. Med.* **2020**, *23*, 102087.
[6] H. Crawford, M. Dimitriadi, J. Bassin, M. T. Cook, T. F. Abelha, J. Calvo-Castro, *Chem.–A Eur. J.* **2022**, *28*, e202202366.
[7] N. Yang, M. Weinfeld, H. Lemieux, B. Montpetit, I. S. Goping, *Cell Death Dis.* **2017**, *8*, e2587–e2587.
[8] L. Ruan, M. Zhou, J. Chen, H. Huang, J. Zhang, H. Sun, Z. Chai, Y. Hu, *Chem. Commun.* **2019**, *55*, 14645–14648.
[9] C. Gianpiero, D. Anis, R. Aikaterini, T. Eirini, V. S. Ioannis, F. G. Dimitrios, T. John, *Medchemcomm* **2017**, *8*, 67–72.
[10] M. V. Dubinin, A. A. Semenova, A. I. Ilzorkina, N. V. Penkov, D. A. Nedopekina, V. A. Sharapov, E. I. Khoroshavina, E. V. Davletshin, N. V. Belosludtseva, A. Y. Spivak, K. N. Belosludtsev, *Free Radic. Biol. Med.* **2021**, *168*, 55–69.
[11] C. A. Kulkarni, B. D. Fink, B. E. Gibbs, P. R. Chheda, M. Wu, W. I. Sivitz, R. J. Kerns, *J. Med. Chem.* **2021**, *64*, 662–676.
[12] M. S. A. Windsor, M. Busse, D. E. Morrison, R. W. Baker, L. R. Hill, L. M. Rendina, *Chem. Commun.* **2021**, *57*, 8806–8809.
[13] N. Magalhães, G. M. Simões, C. Ramos, J. Samelo, A. C. Oliveira, H. A. L. Filipe, J. P. P. Ramalho, M. J. Moreno, L. M. S. Loura, *Molecules* **2022**, *27*, 1420–1439.
[14] J. B. Grimm, A. N. Tkachuk, R. Patel, S. T. Hennigan, A. Gutu, P. Dong, V. Gandin, A. M. Osowski, K. L. Holland, Z. J. Liu, T. A. Brown, L. D. Lavis, *J. Am. Chem. Soc.* **2023**, *145*, 23000–23013.
[15] V. M. Runge, *Invest. Radiol.* **2017**, *52*, 317–323.
[16] T. Grobner, *Nephrol. Dial. Transplant.* **2006**, *21*, 1104–1108.
[17] S. L. Ho, H. Yue, T. Tegafaw, M. Y. Ahmad, S. Liu, S.-W. Nam, Y. Chang, G. H. Lee, *ACS Omega* **2022**, *7*, 2533–2553.
[18] E. Baubeta, E. Laurin Gadsböll, L. Will, F. Holmquist, M.-L. Aurumskjöld, *J. Appl. Clin. Med. Phys.* **2024**, *25*, e14324.
[19] K. W. Van Delinder, R. Khan, J. L. Gräfe, *Sci. Rep.* **2020**, *10*, 13417.
[20] A. G. Robertson, L. M. Rendina, *Chem. Soc. Rev.* **2021**, *50*, 4231–4244.
[21] A. J. Hall, A. G. Robertson, R. W. Baker, L. R. Hill, L. M. Rendina, *Chem. Commun.* **2023**, *59*, 12511–12514.
[22] D. E. Morrison, J. B. Aitken, M. D. de Jonge, F. Issa, H. H. Harris, L. M. Rendina, *Chemistry* **2014**, *20*, 16602–16612.
[23] A. J. Hall, A. G. Robertson, L. R. Hill, L. M. Rendina, *Sci. Rep.* **2021**, *11*, 598.
[24] C. Rivas, G. J. Stasiuk, J. Gallo, F. Minuzzi, G. A. Rutter, N. J. Long, *Inorg. Chem.* **2013**, *52*, 14284–14293.
[25] J.-S. Wu, I.-C. Hwang, K. S. Kim, J. S. Kim, *Org. Lett.* **2007**, *9*, 907–910.
[26] T. Nguyen, M. B. Francis, *Org. Lett.* **2003**, *5*, 3245–3248.
[27] T. Alexandrov, *BMC Bioinf.* **2012**, *13*, S11.
[28] M. Ghasemi, T. Turnbull, S. Sebastian, I. Kempson, *Int. J. Mol. Sci.* **2021**, *22*, 12827–12857.
[29] P. K. Magut, S. Das, V. E. Fernand, J. Losso, K. McDonough, B. M. Naylor, S. Aggarwal, I. M. Warner, *J. Am. Chem. Soc.* **2013**, *135*, 15873–15879.
[30] P. Wang, F. Qin, L. Wang, F. Li, Y. Zheng, Y. Song, Z. Zhang, W. Cao, *Opt. Express* **2014**, *22*, 2414–2422.
[31] R. N. Dsouza, U. Pischel, W. M. Nau, *Chem. Rev.* **2011**, *111*, 7941–7980.
[32] X. Liu, Q. Qiao, W. Tian, W. Liu, J. Chen, M. J. Lang, Z. Xu, *J. Am. Chem. Soc.* **2016**, *138*, 6960–6963.
[33] J. Dai, X. Zhang, *Chemical and Biomedical Imaging* **2023**, *1*, 796–816.

Manuscript received: June 10, 2024
Accepted manuscript online: July 24, 2024
Version of record online: ■■, ■■

RESEARCH ARTICLE

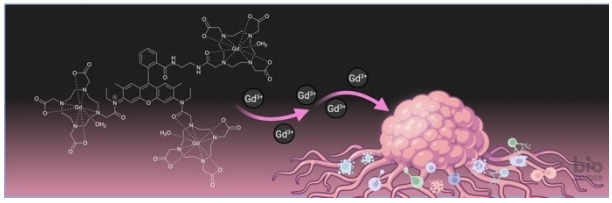

*A. G. Robertson, A. J. Hall, A. Marfavi, L. M. Rendina**

Superior cell uptake and tumor cell selectivity at low incubation concentrations by new mono- and tri-nuclear rhodamine-gadolinium(III) agents are reported, offering potential dual MRI/fluorescent probes for advanced theranostic applications.